1997 International Solar Energy Conference. Proceedings. April 27-30, 1997, Washington, DC. Sponsored by the Solar Energy Division, ASME. Edited by David E. Claridge, James E. Pacheco. The American Society of Mechanical Engineers, New York, NY. 1997

Field Performance of Photovoltaic Solar Water Heating Systems

A. Hunter Fanney, ASME Fellow
Brian P. Dougherty, ASME Associate Member
Kenneth P. Kramp, ASME Student Member

Building Environment Division
National Institute of Standards and Technology

Abstract

Energy consumed for water heating accounts for approximately 17 quads of the energy consumed by residential and commercial buildings. Although there are over 90 million water heaters currently in use within the United States (Zogg and Barbour, 1996), durability and installation issues as well as initial cost have limited the sales of solar water heaters to less than 1 million units. Durability issues have included freeze and fluid leakage problems, failure of pumps and their associated controllers, the loss of heat transfer fluids under stagnation conditions, and heat exchanger fouling. The installation of solar water heating systems has often proved difficult, requiring roof penetrations for the piping that transports fluid to and from the solar collectors. Fanney and Dougherty have recently proposed and patented a solar water heating system that eliminates the durability and installation problems associated with current solar water heating systems. The system employs photovoltaic modules to generate electrical energy which is dissipated in multiple electric heating elements. A microprocessor controller is used to match the electrical resistance of the load to the operating characteristics of the photovoltaic modules. Although currently more expensive than existing solar hot water systems, photovoltaic solar water heaters offer the promise of being less expensive than solar thermal systems within the next decade. To date, photovoltaic solar water heating systems have been installed at the National Institute of Standards and Technology in Gaithersburg, MD and the Florida Solar Energy Center in Cocoa, FL. This paper will review the technology employed, describe the two photovoltaic solar water heating systems, and present measured performance data.

Introduction

A photovoltaic solar water heating system, Figure 1, has been developed and patented by the National Institute of Standards and Technology (Fanney and Dougherty, 1994). Unlike the other residential applications of photovoltaic modules, this system does not require an inverter to convert the direct current supplied by the photovoltaic array to an alternating current or use a battery system for storage. The system does not require a minimum solar irradiance level to operate, all incident solar energy is converted to electrical energy and delivered to the storage tank. Finally, there are no electric

interconnections between the photovoltaic system and the electric utility.

SOLAR PHOTOVOLTAIC HOT WATER SYSTEM

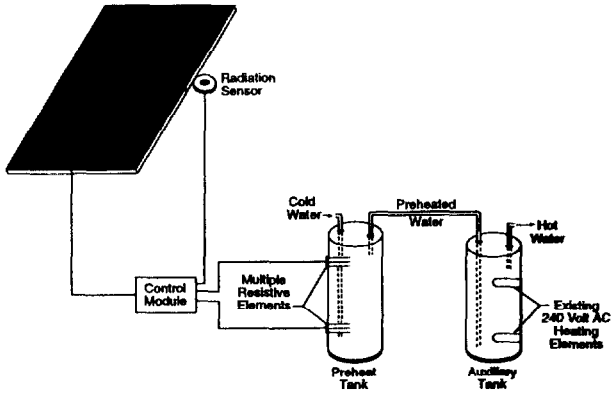

Figure 1

The major components of the system are an array of photovoltaic modules, a microprocessor controller, and a storage tank(s) that contains multiple electrical heating elements. The microprocessor controller connects the individual heating elements in various combinations such that the photovoltaic array continuously operates at or near maximum efficiency. The process is illustrated in Figure 2 in which the current versus voltage curves for two solar irradiance levels, 200 and 1000 W/m^2 are shown for a representative photovoltaic array. There is a point on each curve at which the product of the current and voltage gives the maximum power output, P_{max}. In order to obtain maximum power output from the photovoltaic array, the electrical resistance of the load must correspond to the maximum power point or, in terms of the graph in Figure 2, must be on the load line that passes through the maximum power point. For the example given, an electrical resistance of 13 ohms passes through the maximum power point at an irradiance of 1000 W/m^2. However, as the irradiance deviates from 1000 W/m^2, the 13 ohm load line no longer coincides with the maximum power point. For example, at an irradiance of 200 W/m^2, a level typical of early morning and late afternoon hours, the power output of the photovoltaic array depicted in Figure 2 would be 100 watts. If the resistive load were 67 ohms instead of 13 ohms, however, the photovoltaic array would operate at the maximum power point for the 200 W/m^2 irradiance level resulting in a power output of 445 watts. Thus, in order to capture the maximum possible energy for all meteorological conditions, a variable resistive load is needed. It has been assumed that the module temperature is constant for this illustrative example. The influence of module temperature on the operating characteristics of a photovoltaic module is significantly less than that of solar irradiance.

PHOTOVOLTAIC ARRAY CURRENT VERSUS VOLTAGE CHARACTERISTICS
4 Parallel Strings of 10 Panels in Series

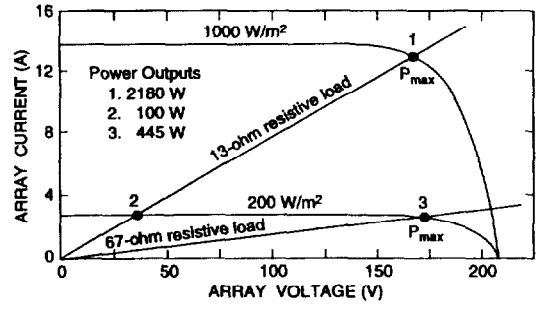

Figure 2

Since the use of a single heating element with variable resistance is not practical, the photovoltaic solar water heating systems described in this paper use multiple electric heating elements connected in various configurations to approximate a variable resistive load. A microprocessor controller continuously connects the individual heating elements in various manners such that the resulting load line always passes through or near the photovoltaic array's maximum power point. An analysis (Fanney and Dougherty, 1996) has shown that the use of as few as three heating elements can capture 94 percent of the maximum possible energy.

A photovoltaic solar water heater may be configured as a single-tank or two-tank system. In a single-tank configuration, water within the lower portion of the tank is heated by energy from the photovoltaic modules whereas the upper portion of the tank is heated by a utility connected resistive element. The single-tank system's design, specifically the location

of the auxiliary heating element, must ensure that an adequate hot water supply is available during unfavorable solar conditions. In a two-tank configuration, water within the preheat tank is heated by the photovoltaic array, whereas the water stored in the second, or auxiliary, tank, is heated by resistive elements connected to the electric utility or by a fossil-fuel burner if a gas or oil water heater is used. A detailed discussion of the costs and advantages/disadvantages of the system relative to solar thermal hot waters are included in previous work (Fanney and Dougherty, 1996). This previous work showed that in order for photovoltaic solar water heating systems to be competitive with solar thermal hot water systems, photovoltaic cell costs must decline from the current price of $5.00 to $1.90 per peak watt. This paper describes two full scale demonstration systems and presents performance data for each system.

System Description and Instrumentation

This paper reports on the performance of photovoltaic solar water heating systems located in Gaithersburg, Maryland (latitude 39.1) and Cocoa, Florida (latitude 28.4). The Maryland site is located at the Building and Fire Research Laboratory within the National Institute of Standards and Technology (NIST). The system at Cocoa, Florida is being evaluated at the Florida Solar Energy Center (FSEC). System specifications are given in Table 1.

Each photovoltaic module consists of 36 single crystal solar cells connected in series. The rated power output of each module is 53 watts at a solar irradiance of 1000 W/m^2 and a cell temperature of 25 °C. The photovoltaic array at the NIST site consists of 30 modules. The modules are interconnected in a manner that results in three parallel strings of 10 modules connected in series. At the rating conditions noted above, this array produces approximately 1590 watts at a current and voltage of 9.1 amps and 174 volts, respectively. The photovoltaic water heating system at the FSEC site uses three parallel strings of nine modules connected in series, resulting in a rated power output of 1431 watts at approximately 9.1 amps and 157 volts.

The photovoltaic solar hot water systems at both sites use a two-tank configuration. The tanks are piped in series with the preheat tank being upstream of the auxiliary tank as shown in Figure 1. During a draw, water is removed from the top of the auxiliary tank, water from the top of the preheat tank is fed to the bottom of the auxiliary tank, and water from the cold water main inlet is supplied to the bottom of the preheat tank. The preheat tank is a nominal 302 liter residential water heater in which the upper and lower 4500 watt heating elements have been replaced with an assembly having three individual heating elements, Figure 3. The six replacement elements are used in combination with the photovoltaic array to heat the water within this preheat tank. The auxiliary tank is a nominal 190 liter residential electric water heater having two interlocked 4500 watt heating elements. For both the NIST and FSEC systems, the six, preheat tank resistive elements are wired in parallel.

Figure 3

Although six, parallel-wired elements provide the opportunity for a maximum of 63 discrete resistive loads, both systems were limited to using only six load combinations. This decision was made because six properly selected elements can result in an annual photovoltaic array energy output that is only 4 to 6 percent lower than the theoretical performance obtained using a continuously variable resistor (Fanney and Dougherty, 1996). Only a minimal improvement in performance is obtained by using the other 57 load combinations (see later section, "Hypothetical System 3"). Wiring configurations that allow both parallel and series combinations are available but at the cost of a more complex wiring layout and the need for additional power relays.

The control logic used by the two field systems is simple, with the choice of the connected resistive load

Table 1
Photovoltaic Solar Hot Water System Specifications

System Location	NIST Gaithersburg, Maryland	FSEC Cocoa, Florida
Latitude	39.1°	28.4°
Longitude	77.2°	80.8°
Tilt	40°	24.0°
Azimuth	0.0°	0.0°
Photovoltaic Array Size (m^2)	12.8	11.5
Number of Modules in Series	10	9
Number of Module Stings in Parallel	3	3
Nominal/Actual Preheat Tank Volume (l)	303/272.4	303/272.4
Nominal/Actual Auxiliary Tank Volume (l)	190/170.4	190/170.5
Auxiliary Tank Thermostat Set Point (°C)	57.0	51.7
Preheat Storage Tank Heat Loss Coefficient (W/°C)	1.92	2.17
Auxiliary Storage Tank Heat Loss Coefficient (W/°C)	1.21	1.43
Preheat Tank Upper Heating Elements: Nominal Resistance (Ω) Operating Sequence	180-1 120-5 75-6	120-1 120-5 120-6
Preheat Tank Lower Heating Elements Nominal Resistance (Ω) Operating Sequence	180-2 110-3 75-4	90-2 90-3 110-4
Solar Irradiance Range, H_T (W/m^2) For Each Nominal Resistive Load (Ω)	180.0: $0 \le H_T < 138$ 90.0: $138 \le H_T < 273$ 49.5: $273 \le H_T < 483$ 29.8: $483 \le H_T < 687$ 23.9: $687 \le H_T < 882$ 18.1: $882 \le H_T$	120.0: $0 \le H_T < 200$ 51.4: $200 \le H_T < 385$ 32.7: $385 \le H_T < 540$ 25.2: $540 \le H_T < 675$ 20.8: $675 \le H_T < 800$ 17.7: $800 \le H_T$

combination depending only on the measured irradiance . As implied by Figure 2, at the lowest irradiances, the highest resistive load yields the highest output. At the highest irradiances, the lowest resistive load is used. Given the parallel wiring arrangement, the highest resistive load is achieved by having only the first element connected. As irradiance increases, the other heating elements are sequentially connected in parallel. The sequencing, placement, and nominal ohm ratings of the individual heating elements, plus the irradiance range over which each load combination is used, are listed in Table 1. Because the control logic calls for resistive element number 1 to be connected at all times, it is hard-wired to the array. The irradiance range corresponding to each resistive load combination is determined during system design. The procedure used for selecting the irradiance ranges and the individual heating elements is described elsewhere (Fanney and Dougherty, 1996, Williams, 1996).

A microprocessor controller, which is programmed to execute the logic for selecting the appropriate resistive load, measures irradiance and uses digital output channels to energize the appropriate DC power relays. A reference cell, which is mounted with the array is used as the radiation sensor. The reference cell's output was calibrated using a pyranometer prior to installation. For the NIST installation, control logic is repeated every 20 seconds. At the FSEC site, resistive load changes are considered every minute

based on the average of 3 irradiance measurements made during the minute. Alternative options for the radiation sensor and controller are described in the patent (Fanney et al., 1994). Examples of how the controller changes the resistive load over the course of a clear and an intermittently cloudy day are shown in Figures 4 and 5, respectively.

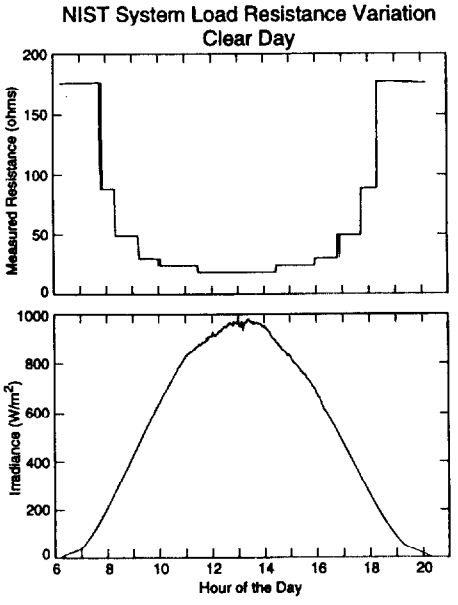

Figure 4

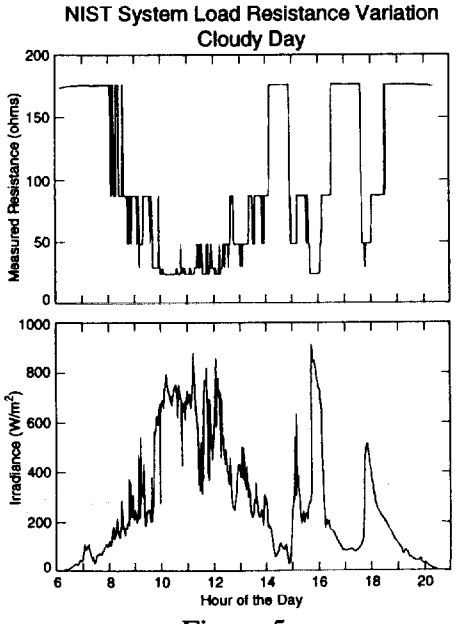

Figure 5

The instrumentation used to measure the performance of both systems is identical. A pyranometer is used to measure the solar irradiance incident upon each photovoltaic array. The power output of the photovoltaic array is determined by measuring the array's output voltage and current. A watt transducer is used to measure the auxiliary tank's electrical energy consumption.

Temperature measurements are made using type-T thermocouples. Temperature measurement locations include: the indoor and outdoor ambient, the temperature of the water as it enters and leaves each storage tank, and the temperature of the water at six vertical locations within each storage tank. Two measurements are made to quantify the amount of hot water removed from the system during a hot water draw, a pulse generating integrating-type water meter and a load cell that measures the mass of water withdrawn. The load cell is used as the primary measurement.

The output signal of each transducer is measured by a data acquisition system interfaced with a personal computer. All transducers are scanned every minute. Whenever hot water is removed, the inlet and outlet temperatures at each storage tank, the water meter, and the load cell are measured every six seconds. The personal computer converts the measured quantities into engineering units and stores the data on diskettes for final analysis. The personal computer also initiates the hot water draws. Prior to the selected draw hours, the computer issues a command to the data acquisition system to close a drain valve located at the bottom of a weigh tank and make a pre-draw mass measurement. At the beginning of the draw hour, a valve at the exit of the auxiliary tank is opened by the data acquisition system. The draw continues until the volume of water removed is equal to the desired quantity. Upon reaching the specified volume, the computer terminates the draw, weighs the tank, and subsequently opens the drain valve on the weigh tank.

Field Performance Results

The primary objective of this study was to determine the thermal performance of solar photovoltaic hot water systems subjected to different climatic conditions. Identical hot water removal schedules were used at both sites. The quantity of hot water removed each day, 243 liters, is equivalent to that specified within the Department of Energy's test procedure for residential water heaters (Federal Register, 1990). The daily draw schedule consists of 20.5 liters withdrawn at 6:00 a.m. and 6:00 p.m., 61 liters at 7:00 a.m. and 7:00 p.m., and 40.5 liters at 8:00 a.m. and 8:00 p.m. This daily draw schedule is based on the American Society of Heating, Refrigerating, and Air-Conditioning Engineers Inc. Standard 137-95 (ASHRAE 1995) for evaluating combined heat pump-water heating appliances. Secondary objectives were to provide experimental data for computer model validation, to determine the influence of alternative control strategies on system performance, and to quantify the number of relay toggles associated with each strategy. Twelve months of data have been analyzed for both the NIST and FSEC systems.

One storage tank at both NIST and FSEC had to be replaced during the data collection period because of a leak. The leaks were attributed to the combination of small manufacturing defects being exacerbated to the point of failure by the removal of the anode rod in favor of the in-tank temperature probes. (Hot water port anode rods will be used in future cases where in-tank temperature probes are used.) In addition to the down-time required for replacing the leaking tank, FSEC data losses have occurred because of losses of supply water, to modify wiring to avoid a floating voltage measurement, and to correct for the leap day. Additional data were lost at NIST for one to several hours as the result of troubleshooting instrumentation, printer jams, operator errors, and interruptions resulting from connecting additional instrumentation. In the "Field Performance Results" section that follows, no data were eliminated during time intervals that the array and outdoor instrumentation were covered with snow or ice. Data from periods of snow coverage, however, were excluded from the data sets used for validating computer models. The use of data from days where a partial data loss occurred can cause potential distortions, both negative and positive, of the system's performance and, in general, makes the data analysis more difficult and subjective. Thus, in this paper, days where a portion of data was lost were excluded when compiling the final data sets. Given this criteria, the resulting field performance data capture rates for each month are listed in Tables 2 and 3 for the NIST and the FSEC sites, respectively. For the overall monitoring periods, 94.5 percent of the days from the NIST site and 94.0 percent of the days from the FSEC site have been used for analysis.

The field measured performance of the NIST and FSEC photovoltaic solar water heating systems are summarized in Tables 2 and 3, respectively. Solar fraction and electrical fraction provide two measures for readily evaluating the performance of the overall system. Solar fraction is defined as the ratio of the energy removed from the preheat tank to the total energy removed from the system as a result of hot water draws. These energy draw quantities, which appear in Tables 2 and 3, are determined by integrating the product of the incremental mass removed, the specific heat of the withdrawn water, and the difference between the leaving and entering water temperatures during hot water draws. Solar fraction is the measurement traditionally used to assess the performance of solar thermal hot water systems.

A secondary performance measure used in this study is electrical fraction. The electrical fraction is defined as the ratio of electrical energy supplied to the preheat tank from the photovoltaic array to the electrical energy used by the auxiliary tank. Electrical fraction may be used exclusively for future field studies as the quantities required are easier to measure than the quantities needed to compute solar fraction.

The monthly solar and electrical fractions for the NIST system are given in Figure 6 and Table 2. Solar fractions ranged from a low of 21.5 percent in January 1996 to a high of 60.5 in August, 1995. The relatively

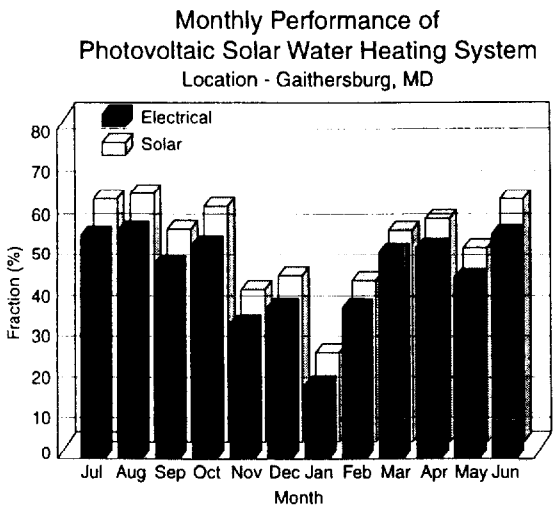

Figure 6

poor performance in January 1996 is attributed to a series of snowfalls that left the array completely buried for seven consecutive days and, to varying degrees, partially covered for the 5 days that followed. For the 12-month monitoring period, the overall solar fraction was 48.0 percent. The 12-month electrical fraction, by comparison, was 44.6 percent.

The performance of the FSEC system is summarized in Figure 7 and Table 3. The solar fraction varied from 50.8 percent, December 1995, to 91.6 percent for the month of July 1996. The overall solar and electrical fractions were 72.8 and 67.0 percent, respectively. For a total of 12 days during the peak months of May to August, no auxiliary heating occurred. The monthly photovoltaic array efficiencies, electrical power output divided by the product of incident solar energy and photovoltaic array area, are plotted for both test sites in Figure 8. It should be noted that the reported conversion efficiency includes the effect that the resistive loads do not always coincide with the photovoltaic array's maximum power point. For the NIST site, the twelve month array efficiency was 11.0 percent. By comparison, the FSEC site average array efficiency for the 12-month monitoring period was 10.0 percent. This lower conversion efficiency is attributed to three factors: (1) the comparatively higher module operating temperatures at the FSEC site, (2) the fact that the irradiance ranges used for each load combination were modified at the NIST site after having collected in-situ, resistive load data, (3) controller decisions on whether to change the resistive load combination were made less frequently at FSEC, and (4) the pyranometer at the NIST site, which was used to measure the incident solar energy flux, occasionally was completely covered by snow while the array itself was only partially covered.

The impact of this last factor is that the array was generating power, albeit at a diminished rate, while the incident solar energy flux was recorded as being zero when, in fact, it was non-zero. Following the digging out process from the heavy snows of January, the researchers made an effort to clear both the array and the outdoor instrumentation as soon as possible following the snowfalls in February and March.

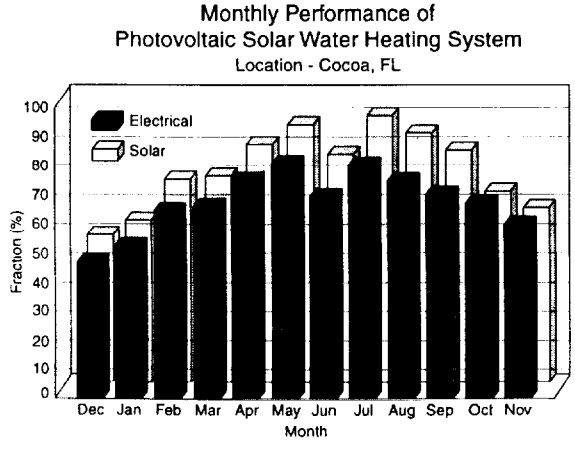

Figure 7

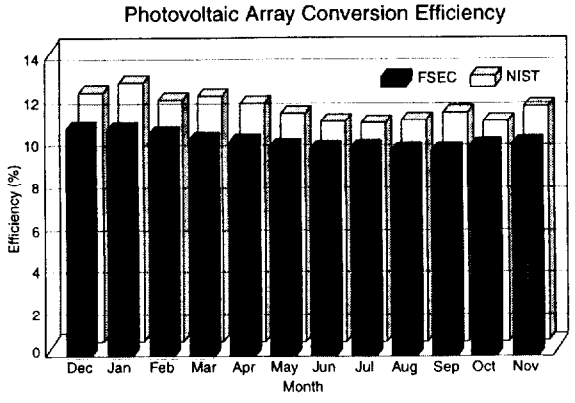

Figure 8

Table 2
Monthly Performance of Photovoltaic Solar Water Heating System
Location - Gaithersburg, MD

Month	Year	Data Capture Rate	Incident Solar Energy	Photovoltaic Array Output	Photovoltaic Array Efficiency	Electric Energy Supplied to Auxiliary Tank	Energy Removed From Preheat Tank	Energy Removed From System	Heat Loss From Preheat Tank	Heat Loss From Auxiliary Tank	Solar Fraction	Electrical Fraction
		(%)	(kJ/m²)	(kJ)	(%)	(kJ)	(kJ)	(kJ)	(kJ)	(kJ)	(%)	(%)
JUL	1995	87.1	562328	736341	10.2	604446	721409	1216390	27649	93405	59.3	54.9
AUG	1995	100.0	647127	862964	10.4	676781	847170	1399708	30703	106566	60.5	56.0
SEP	1995	100.0	512342	704227	10.7	776938	700317	1351034	17003	102699	51.8	47.5
OCT	1995	100.0	548020	793635	11.3	731053	797201	1395462	25018	106264	57.1	52.1
NOV	1995	96.7	317170	477758	11.8	969377	488803	1332569	-6342	99322	36.7	33.0
DEC	1995	87.1	332928	504185	11.8	868031	512892	1282418	657	93516	40.0	36.7
JAN	1995	96.8	168470	263071	12.2	1198336	298368	1387792	-27395	102807	21.5	18.0
FEB	1995	96.6	355576	516734	11.4	883095	496910	1283969	-3195	96288	38.7	36.9
MAR	1996	80.6	432540	640549	11.6	633593	577868	1125314	9500	85874	51.4	50.3
APR	1996	90.0	474610	679244	11.2	647526	646284	1195860	13181	92335	54.0	51.2
MAY	1996	100.0	493445	675122	10.7	869043	661856	1407589	4665	105769	47.0	43.7
JUN	1996	100.0	606010	801966	10.3	668160	790754	1344696	22627	102510	58.8	54.6
Annual		94.5	5450566	7655796	11.0	9526379	7539832	15722801	114071	1187355	48.0	44.6

Alternative Control Strategies

A great deal of flexibility exists in the design and control of a photovoltaic solar hot water system. Among the control choices are: the number of resistive elements connected to the photovoltaic array, the number of resistor configurations to be used, the input parameters to the microprocessor controller, and the frequency of control logic decisions.

Experimentally quantifying the effect of various control strategies on system performance is not feasible due to variable weather conditions. Instead, hypothetical control strategies were modeled as the actual photovoltaic water heating system operated. The modeling was done in real time, as opposed to acquiring the needed data and subsequent modeling. Modeling in real time gave researchers an opportunity to change the control strategy used by the actual solar photovoltaic hot water system if an alternate one proved superior. One of the modeled systems was an ideal system that always operates at the photovoltaic array's maximum power point. The results were used to compute the controller performance index, defined as the ratio of the electrical energy produced by each hypothetical system to the energy delivered by an ideal system. A computer simulation tool was developed to model the photovoltaic array, controller, and resistive elements of the NIST system and several hypothetical systems. Weather data supplied to the model were values recorded while monitoring the NIST system. The electrical energy produced by the photovoltaic array of each hypothetical system is calculated using a single-diode four parameter model (Duffie and Beckman, 1991).

TABLE 3
Monthly Performance of Photovoltaic Solar Water Heating System
Location - Cocoa, FL

Month	Year	Data Capture Rate (%)	Incident Solar Energy (kJ/m^2)	Photovoltaic Array Output (kJ)	Photovoltaic Array Efficiency (%)	Electric Energy Supplied to Auxiliary Tank (kJ)	Energy Removed From Preheat Tank kJ)	Energy Removed From System kJ)	Heat Loss From Preheat Tank (kJ)	Heat Loss From Auxiliary Tank kJ)	Solar Fraction (%)	Electrical Fraction (%)
DEC	1995	93.5	402979	495835	10.7	561051	460438	905695	44971	102484	50.8	46.9
JAN	1996	100.0	491684	607320	10.7	544615	552753	992167	51683	110904	55.7	52.7
FEB	1996	100.0	550664	666870	10.5	367054	626603	895864	60325	101156	69.9	64.5
MAR	1996	96.8	611164	721054	10.2	369825	655700	924128	65257	103975	71.0	66.1
APR	1996	76.7	494232	573369	10.1	191505	524391	639744	58668	76207	82.0	75.0
MAY	1996	100.0	673687	757329	9.8	177073	670472	755481	87487	97458	88.7	81.0
JUN	1996	100.0	563467	628248	9.7	247242	555283	707977	77084	93860	78.4	71.8
JUL	1996	83.9	548605	614913	9.7	133916	540068	589902	76803	80441	91.6	82.1
AUG	1996	93.5	560517	618882	9.6	178757	559099	653511	80614	89254	85.6	77.6
SEP	1996	100.0	553640	614453	9.6	232720	549492	690128	76309	91147	79.6	72.5
OCT	1996	100.0	532979	616630	10.0	320481	549142	769402	70773	96067	71.4	65.8
NOV	1996	83.3	405712	470832	10.1	312063	450079	675889	48110	77502	66.6	60.1
Annual Summary		94.0	6389330	7385735	10.0	3636302	6693431	9199887	798084	1120453	72.8	67.0

A description of each hypothetical system and the resulting controller performance index follows:

Actual System

This system is identical in components and control logic to the NIST photovoltaic solar hot water system, Table 1. The predicted annual controller performance index, 96.3, is in excellent agreement with the 96.8 value calculated using the field measured photovoltaic array output. Thus, the model was deemed adequate to explore various control strategies.

Hypothetical System 1

The controller in this system calculated the solar irradiance using the reference cell's short circuit current, temperature, and an equation supplied by the reference cell's manufacturer. The annual predicted controller performance index was 96.1, which is slightly lower than versus the 96.3 value predicted when the reference cell temperature was ignored. This difference is attributed to the fact that the reference calibration cell at NIST was conducted over a wide range of weather conditions compared to the manufacturer's calibration conducted at standard rating conditions.

Hypothetical System 2

The control logic used in this system takes into account the influence of temperature on photovoltaic array efficiency when selecting the most appropriate combination of heating elements. The array temperature effect is neglected by the other systems. The resulting annual controller performance index is 96.5, 0.2 more than the actual system's value.

Hypothetical System 3

Six heating elements are connected in various parallel combinations resulting in 17 discrete levels of load resistance. This system used both the reference cell's short circuit current and temperature to compute

solar irradiance and thus should be compared to Hypothetical System 1, which like both field sites, only used six load options. The results show that increasing the number of discrete resistive loads from 6 to 17 resulted in only a modest improvement, 96.1 to 97.3, in the annual controller performance index.

Hypothetical System 4

This system employed three heating elements connected in various configurations resulting in seven discrete levels of load resistance. The solar irradiance was measured in a manner identical to Hypothetical Systems 1 and 3. The resulting controller index, 96.0, is 0.1 less than that observed for the systems which employed six discrete levels of load resistance, Hypothetical System 1, and 1.3 lower than observed when 17 discrete levels of load resistance are used, Hypothetical System 3.

Hypothetical System 5

The control logic used in this system measures solar irradiance and connects the selected resistive elements every two minutes rather than every 20 seconds as is done in the actual system's control logic.

This system was added after two months of system operation. The results for the ten month interval decrease from 96.2 to 95.0 percent due to the slower sampling rate.

These results show that neglecting the photovoltaic array's temperature within the control strategy had negligible effect on the photovoltaic solar hot water system's overall performance. The additional complexity associated with increasing the number of discrete load resistance levels from six, used in the NIST and FSEC systems, to 17 appears unwarranted in view of the modest improvement in system performance. In fact, the use of only three elements configured in a manner to yield seven levels of load resistance resulted in overall performance within 0.1 percent of the value obtained using a six element configuration. Finally, it is interesting to note that the effect of decreasing the frequency at which control logic decisions are made from three times a minute to once every two minutes had an effect equal in magnitude to the other options considered.

Power relays are used to connect the individual heating elements to the photovoltaic array upon receiving a control signal from the microprocessor. In order to predict the expected relay life, the computer program used to determine the hypothetical system's controller performance index also calculated the number of cycles experienced by each relay. Each relay has an expected mechanical life of 1×10^7 cycles (Potter & Brumfield, 1993). Table 4 shows the average daily number of cycles experienced by each relay for the hypothetical systems previously described. The greatest number of cycles per day occurs for relays contained within hypothetical systems 3 and 4.

Table 4
Average Daily Relay Closures Associated With The Hypothetical Systems

Configuration	Relay 1	Relay 2	Relay 3	Relay 4	Relay 5	Relay 6
Actual System	N/A	10.7	28.4	40.3	41.3	33.8
System 1	N/A	10.4	23.1	40.0	41.3	33.0
System 2	N/A	10.7	23.3	39.5	40.7	32.7
System 3	132.6	152.5	85.0	60.7	131.2	41.3
System 4	113.2	72.4	40.4	N/A	N/A	N/A
System 5	N/A	7.6	12.7	19.1	18.1	14.3

The highest number of average daily cycles experienced by any relay was 152.5, which translates to an annual total of 55,700. Thus, relay mechanical life is not a design issue. The relay's electrical life expectancy will be addressed in future studies.

Summary and Future Activities

This paper presents long-term thermal performance results for two photovoltaic solar water heating systems. The systems are located at the National Institute of Standards and Technology (NIST) and the Florida Solar Energy Center (FSEC). The monthly solar fraction associated with the NIST system ranged from 21.5 to 60.5 percent. The monthly performance of the FSEC system varied from 50.8 percent to 91.6 percent. An annual solar fraction of 48.0 percent was achieved with the NIST system, whereas an annual solar fraction of 72.8 percent was measured for the FSEC system.

A computer simulation tool was developed and used to evaluate alternative control strategies and to quantify the relationship between the annual solar fraction and the number of discrete resistive values available to the microprocessor controller. The results show that increasing the number of resistive combinations from six, used in the FSEC and NIST systems, to 17 resulted in only a modest improvement in the controller performance index. In fact, the use of only three elements in seven combinations yielded performance results very close, 96.0 versus 96.1, to that obtained using a six element, six load combination configuration. Decreasing the frequency at which control logic decisions are made had as great an effect as increasing the number of resistive element combinations employed to seventeen.

NIST is working with the University of Wisconsin to develop simulation tools to predict the performance of photovoltaic solar water heating systems. The resulting models will be used to size components, provide predictions of system performance, and to conduct life-cycle costs analysis. Predictions of electrical demand reductions and the impact on the environment through the widespread use of these systems will also be modeled.

A single-tank version of the photovoltaic solar water heating system is being developed and fabricated. The single-tank system will be monitored at both the NIST and FSEC sites to provide additional data for model validation. A two-tank photovoltaic solar hot water system was installed in October 1996 at the Great Smoky Mountain National Park. This system, which is sponsored by the Tennessee Valley Authority, will be used to supply hot water to the main visitor's center restroom facilities. Monitoring of the system commenced on November 1, 1996 and will continue for twelve months.

Acknowledgments

The authors would like to express their appreciation to the following NIST personnel who assisted in this study. Donn Ebberts for constructing and instrumenting the two photovoltaic solar water heating systems, Mark Davis for reducing the experimental data, and Paula Svincek for preparing the manuscript for publication.

NIST greatly appreciates the efforts of personnel at the Florida Solar Energy Center. In particular the efforts of Jim Huggins and Roy Coffman for overseeing the installation and keeping a watchful eye on the system, Steve McSorley for installing the photovoltaic array, and Dr. David Block for expressing a keen interest in the project. Without the efforts of these dedicated individuals, it would not have been possible to evaluate the performance of a photovoltaic solar water heating system in Florida.

References

Duffie, J.A. and Beckman, W.A., "Design of Photovoltaic Systems", *Solar Engineering of Thermal Processes*, Second Edition, John Wiley & Sons, Inc., New York, 1991, pp 770-781.

Fanney, A.H. and Dougherty, B.P., "Photovoltaic Solar Water Heating System" United States Patent Number 5,293,447, March, 1994.

Fanney, A.H. and Dougherty, B.P., "A Photovoltaic Solar Water Heating System" *Journal of Solar Energy Engineering*, Accepted for Publication, Aug. 1996.

Fanney, A.H. and Dougherty, B.P., "A Photovoltaic Solar Water Heating System" *Proceedings ASME 1996 International Solar Energy Conference*, San Antonio, Texas, April 1996, pp. 9-18.

Federal Register, Vol. 55, No. 201, October 17, 1990, pp. 42162-42177.

"Methods of Testing for Efficiency of Space-Conditioning/Water-Heating Appliances That Include a Desuperheater Water Heater," *ANSI/ASHRAE Standard 137-95*, ANSI/ASHRAE, Atlanta, GA, 1995.

Technical Databook, Potter & Brumfield, Inc., 1993.

Williams, P.M., "Development and Analysis Tool for Photovoltaic-Powered Solar Water Heating Systems," master's thesis, Mechanical Engineering, University of Wisconsin-Madison, Madison, WI, 1993.

Zogg, R.A. and Barbour, R.A., "Joint Industry/DOE Program to Promote High-Efficiency Water-Heating Technologies," program proposal, 31186, prepared for The Edison Electric Institute and the US Department of Energy, November, 1996.